THE JOURNAL OF COMPARATIVE NEUROLOGY 201:519-539 (1981)

# Visual Topography of V2 in the Macaque

R. GATTASS, C. G. GROSS, AND J. H. SANDELL
*Department of Psychology, Princeton University, Princeton, New Jersey 08544*

*ABSTRACT* The representation of the visual field in the area adjacent to striate cortex was mapped with multiunit electrodes in the macaque. The animals were immobilized and anesthetized and in each animal 30 to 40 electrode penetrations were typically made over several recording sessions.

This area, V2, contains a topographically organized representation of the contralateral visual field up to an eccentricity of at least 80°. The representation of the vertical meridian is adjacent to that in striate cortex (V1) and forms the posterior border of V2. The representation of the horizontal meridian in V2 forms the anterior border of V2 and is split so that the representation of the lower visual field is located dorsally and that of the upper field ventrally. As in V1, the representation of the central visual field is magnified relative to that of the periphery. The area of V2 is slightly smaller than that of V1. At a given eccentricity, receptive field size in V2 is larger than in V1.

The myeloarchitecture of V2 is distinguishable from that of the surrounding cortex. The location of V2 corresponds, at least approximately, to that of cytoarchitectonic Area OB. V2 is bordered anteriorly by several other areas containing representations of the visual field.

In the cat, V2, a cortical area containing a systematic representation of the visual field adjacent to that in striate cortex or V1, was first discovered by Talbot ('42) recording slow potentials. It was later confirmed with single unit recording by Hubel and Wiesel ('65), and recently mapped in detail by Tusa et al. ('79).

In New World monkeys, the existence of a V2 was first suggested by Cowey ('64) in the squirrel monkey and it was subsequently mapped in detail by Allman and Kaas ('74) in the owl monkey. In Old World monkeys (specifically the macaque), Zeki and his colleagues (Zeki and Sandeman, '76; Van Essen and Zeki, '78) have demonstrated a representation of about the central 10° of the lower visual field adjacent to striate cortex. Otherwise, the topographic organization, the extent of visual field represented, and the borders of V2 have not been directly studied with electrophysiological techniques in the macaque.

On the basis of recordings from small groups of neurons, we report on the visual organization of V2 in the macaque. It borders striate cortex and includes a representation of the entire contralateral hemifield. It is myeloarchitectonically distinguishable, and appears to correspond closely to a zone receiving a topographically organized projection from striate cortex (Zeki, '69, '77; Zeki and Sandeman, '76; Cragg, '69; Rockland and Pandya, '81; Ungerleider and Mishkin, '79; Van Essen et al., '79) and to von Bonin and Bailey's ('47) cytoarchitectonic area OB.

A preliminary report of these results has appeared (Gattass et al., '79).

---

J. H. Sandell's present address is Department of Psychology, Massachusetts Institute of Technology, Cambridge, Massachusetts 02139.

R. Gattass's present address is Instituto de Biofisica, Universidade Federal do Rio de Janeiro, R.J., 21910, Brazil.

0021-9967/81/2014-0519$06.00 

## MATERIALS AND METHODS

### *Animal preparation and maintenance*

Seven *Macaca fascicularis* weighing between 3.1 and 4.8 kg were used. Five were recorded from on eight occasions and two twice. All recordings from an individual animal were made within a 4-week period and at least 2 days separated successive recording sessions.

The preparation of the animal for recording and the maintenance and monitoring of the animal during recording have been described in detail previously (Desimone and Gross, '79; Gattass and Gross, '81) and will only be briefly summarized here. Prior to the first recording session a stainless steel well and a bolt for holding the animal in a stereotaxic machine were implanted under aseptic conditions. In each recording session, after injections of atropine and diazepam, the animals were restrained with ketamine hydrochloride, anesthetized with a mixture of halothane, nitrous oxide, and oxygen, immobilized with pancuronium bromide, and maintained under 70% nitrous oxide and 30% oxygen. At the end of each recording session infusion of the paralyzing agent was terminated and after normal breathing returned, the animal was returned to its cage.

### *Recording*

Varnish-coated tungsten microelectrodes with exposed tips of 20–40 μm and 1–6 MΩ impedance were used. They recorded a small number of distinct action potentials. In a typical animal, 30 to 40 vertical electrode penetrations were made over the 4-week recording period. They were spaced approximately 1–2 mm apart forming a grid extending 5–7 mm mediolaterally and 5–7 mm rostrocaudally. Several different cortical areas were usually sampled on each penetration as the electrode was advanced from the dorsal to the ventral surface. On each penetration recording sites were separated by a minimum of 500 μm.

### *Visual stimuli*

The details of the treatment of the eyes and the visual stimuli have been described previously (Gattass and Gross, '81). Briefly, white, colored, and opaque stimuli were presented on a translucent hemisphere located 60 cm from the eye contralateral to the recording sites. The cornea was covered by a contact lens selected by retinoscopy to focus the eye at 60 cm. The ipsilateral eye was occluded.

Since the eye was paralyzed we did not stimulate portions of the retina obscured by the nose and orbital ridge. The extent of our stimulation along the horizontal meridian was about 100° from the vertical meridian, and along the vertical meridian about 55° in the upper visual field and 60° in the lower. Thus, reference to the "complete" visual field or to either "entire" meridian includes only these exposed dimensions.

During each recording session the receptive field boundaries were marked on the hemisphere and subsequently recorded in spherical coordinates as previously described (Sousa et al., '78).

### *Histology*

The histological procedures were described in detail previously (Gattass and Gross, '81). Small electrolytic lesions were made at several recording sites on each penetration by passing a direct current (4 μA for 20 seconds) through the microelectrode. Alternate 33.3-μm frozen sections were stained for cell bodies with cresyl violet and for fibers with one of a variety of stains including a modified Heidenhain-Woelke (Gattass and Gross, '81), Weil ('45), and Spielmeyer (Lillie, '65) stains.

Although both the electrode penetrations and the sectioning of the brain were intended to be vertical, the penetrations never actually fell entirely in a single 33-μm section. Therefore, sites sampled in a single penetration are drawn on coronal (Figs. 7–9), or parasagittal views (Figs. 4–6, 10–12), reconstructed from four to 12 adjacent sections. Furthermore, rows of penetration intended to be in either the same coronal or parasagittal plane sometimes did not remain so throughout their extent. However, such penetrations are represented in the same view. This introduced an error of a maximum of 250 μm in the location of the recording sites.

## RESULTS

### *Visual topography of V2*

In this portion of the Results we first summarize the overall topographic organization of V2. We then illustrate how we delineated the borders of V2 with other visual areas. Finally, we present evidence for the detailed organization of V2. In subsequent portions of the Results, we consider receptive field size and cortical magnification in V2 and then architectonic correlates of V2.

*Overall organization of V2.* Figure 1 summarizes our conclusions on the visual topography of V2. As in V1, receptive fields in V2

recorded on penetrations orthogonal or nearly orthogonal to the cortical surface were located in approximately the same portion of the visual field. The representation of the vertical meridian in V2 is adjacent to that in V1 throughout the latter's extent, i.e., on the lateral surface, on the medial surface, and within the calcarine fissure (at least up to the extent of the representation of the exposed retina) and forms the posterior border of V2. The representation of the horizontal meridian forms the anterior border. The representation of the central 1° in V2 is immediately opposite to that in V1. The representations of the upper and lower visual fields in V2 are separated and each lies anterior to the corresponding representations in V1, the upper visual field ventrally, and the lower visual field dorsally.

Figure 1 is an abstraction of the visual topography of V2 in two ways. First, it is a composite based on the seven animals studied, and there is some variation across animals in the

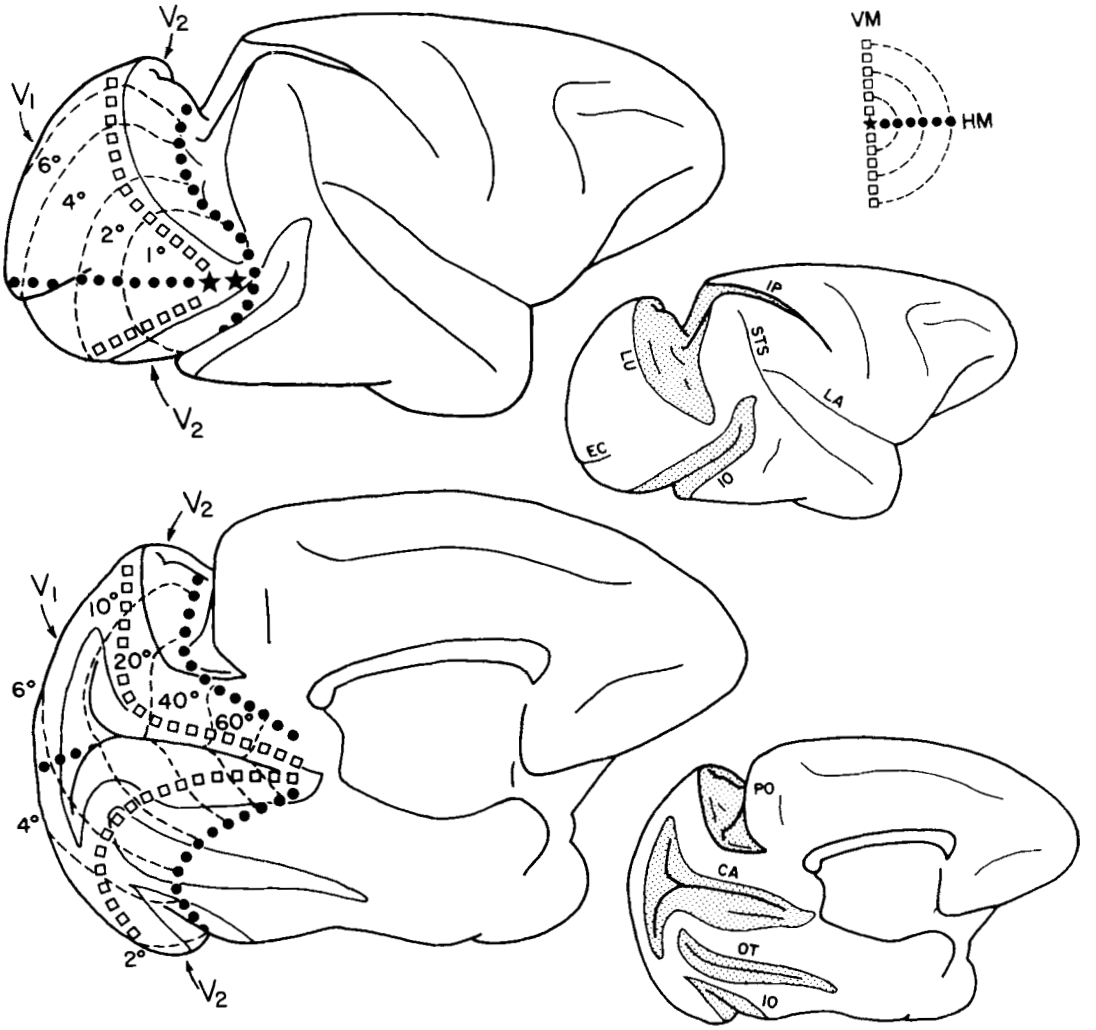


Fig. 1. Visual organization of V2. The drawings are based on photographs of brains in which sulci were partially opened (stippled areas in right drawings). The squares indicate the representations of the vertical meridian (VM), the filled circles the horizontal meridians (HM), and the stars the center of gaze. The dashed lines are isoeccentricity lines. Upper drawings are lateral views and lower ones medial views. The border between V1 and V2 is the representation of the vertical meridian. CA, calcarine sulcus; EC, external calcarine s. IO, inferior occipital s.; IP, intraparietal s.; LA, lateral s.; LU, lunate s.; OT, occipitotemporal s.; PO, parieto-occipal s.; STS, superior temporal s.

location of the meridians with respect to the sulcal pattern. The differences between the visual topography shown on the lateral and medial views of the hemisphere in Figures 8 and 11 are representative of the interanimal variation. Second, the map is based on the average receptive field centers. Thus, the area of the visual field "represented" by a point on the map is larger than that point both because receptive fields have a finite area, and because within a penetration orthogonal to the surface there is some scatter of receptive field location about the point represented on the map. Since both receptive field size and scatter increase with increasing eccentricity, the area in the visual field represented by a point on the map

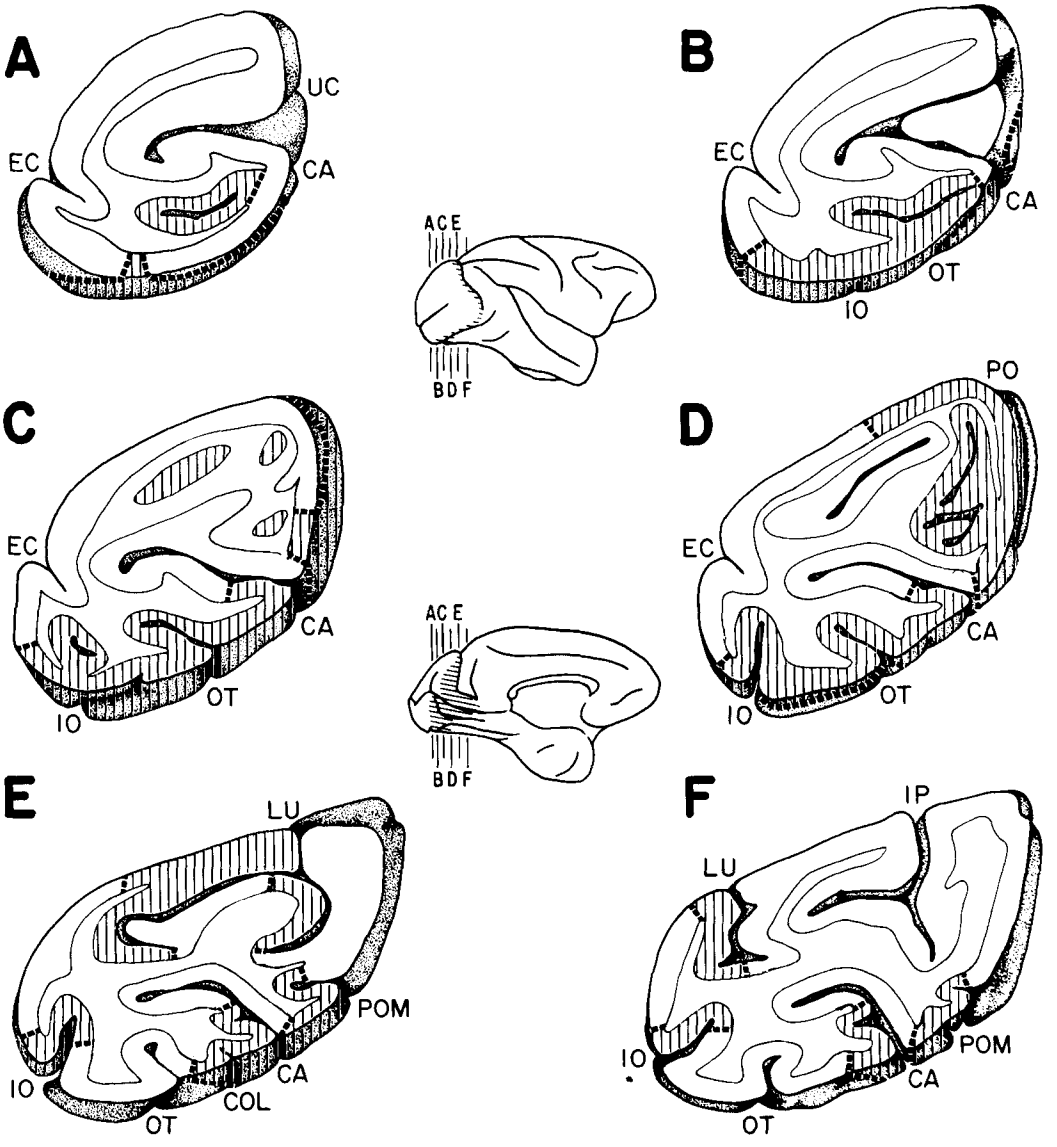


Fig. 2. Extent of V2 (stripes) in contiguous coronal slabs. COL, collateral s.; POM, medial parieto-occipital s.; UC, upper limb of calcarine s. See also legend to Figure 1.

increases with eccentricity. Furthermore, since the map is based on receptive field centers, the extent of the peripheral visual field found to be represented in V2 is greater than that indicated in Figure 1 (even under our conditions of immobilization which obscures the most extreme periphery). Note that the representation of the visual field in V2 extends beyond the region of binocular overlap (approximately 65° according to Kaas et al., '72; Malpeli and Baker, '75). However, the amount of cortex devoted to the monocular crescent is small.

V2 was distinguishable from surrounding areas on myeloarchitectonic criteria. Figure 2 indicates the extent of V2 in an animal whose

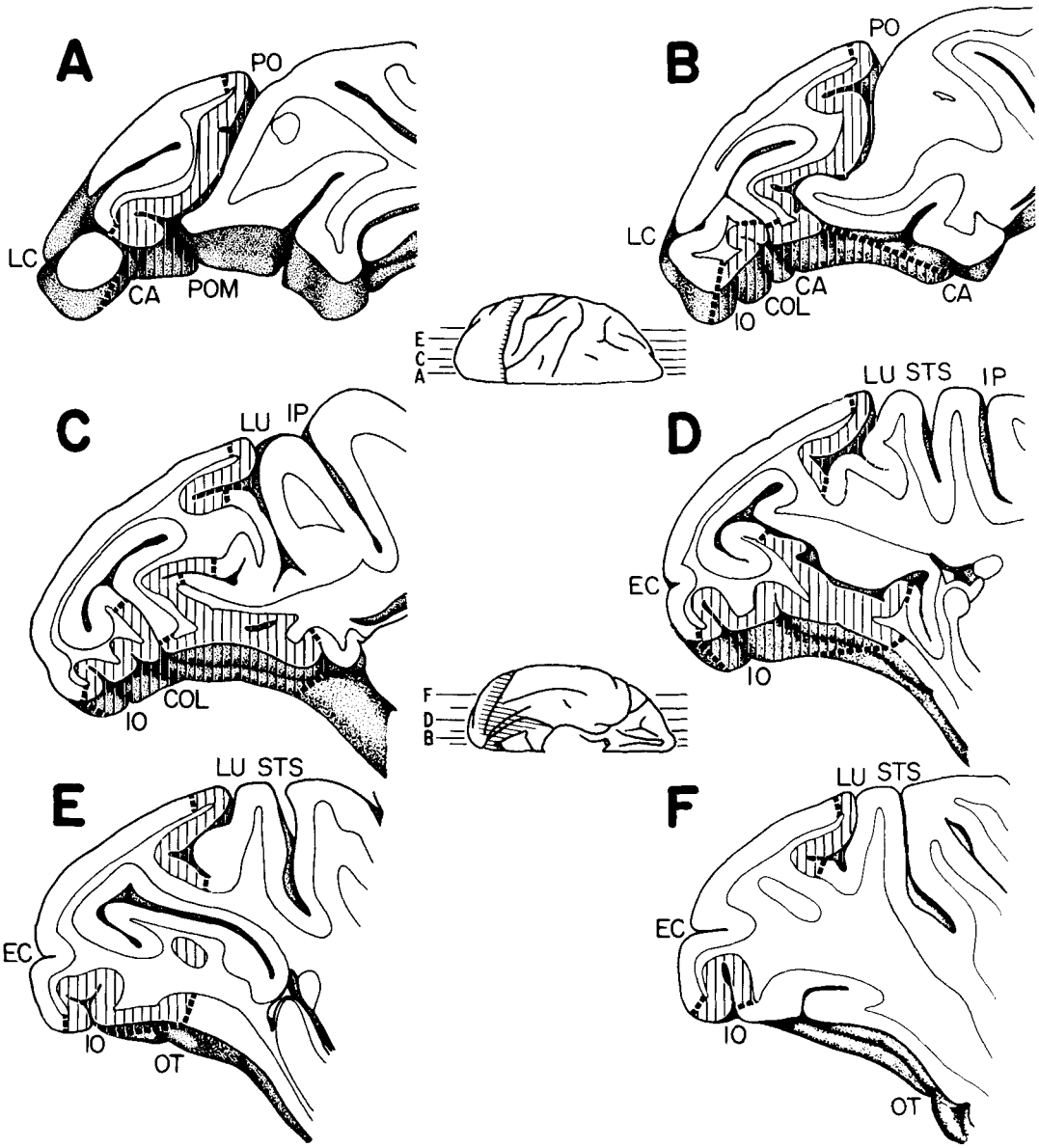


Fig. 3. Extent of V2 (stripes) in contiguous parasagittal slabs. LC, lower limb of calcarine s. See also legend Figures 1 and 2.

brain was sectioned coronally and Figure 3 in one whose brain was sectioned parasagittally. In these figures, the borders of V2 were determined by the myeloarchitectonic criteria described below as well as electrophysiologically. In general, the myeloarchitectonic borders could be determined to within 2 mm, the maximum uncertainty occurring when a border fell in a bend in the cortex. On physiological criteria, the borders could be determined to no closer than about 0.5–2.0 mm, since recording sites on a single penetration were at least 0.5 mm apart and between adjacent penetrations 1–2 mm apart. Within these limits of measurement, the anatomical and physiological border of V2 corresponded.

The area of V1 and V2, determined anatomically and physiologically, was estimated in two animals by measuring the extent of layer IV in 36 sections through V1 and V2 and then multiplying by the distance between the sections. The area estimates, corrected for shrinkage in the histological processing, for V1 were 900 $mm^2$ and 746 $mm^2$, and for V2, 799 $mm^2$ and 660 $mm^2$, respectively. Our estimates for the area of V1 were within the range, but lower than the mean, for a larger series of *M. fascicularis* determined by Van Essen and others (see Van Essen and Maunsell, '80).

*Determination of the borders of V2.* Figures 4–7 illustrate how the borders of V2 were electrophysiologically determined. Each figure illustrates a systematic progression of receptive field locations as the recording sites approach a border of V2 and a reversal of that progression when the border is crossed. In these figures, for simplicity, only about half the actual recording sites are shown.

Figure 4 illustrates the border between V1 and V2 on the ventral surface of the cortex in the area of representation of the central 5° of the upper visual field. Moving in V1 from the dorsal surface to the ventral surface (site 1 to site 6), the receptive fields move from the inferior visual field toward the vertical meridian in the superior visual field. Crossing into V2 and moving anteriorly (site 7 to site 12), the progression reverses and the fields move from the vertical meridian back toward the horizontal meridian. Note that, at similar eccentricities, the fields in V2 tend to be larger than those in V1. Perhaps as a consequence of its larger receptive fields, the topography in V2 is less orderly than in V1.

Figure 5 shows both the posterior and anterior borders of V2 on the dorsal surface in the area of representation of the central 3° of the lower visual field. Moving within V1 toward V2 (site 1 to site 5) the receptive fields progress toward the vertical meridian. Crossing into V2 (site 6) and moving down the posterior bank of the lunate sulcus to site 10 the receptive fields move toward the horizontal meridian. Crossing the anterior border of V2 in the floor of the lunate sulcus we move into another retinotopocally organized area. Moving anteriorly in this area the progression of receptive fields reverses and moves from the horizontal meridian into the periphery of the lower visual field. The location of this area corresponds to that of the dorsal portion of V3 described by Zeki ('78). In this and subsequent figures we have marked receptive field centers that appear to fall within the dorsal portion of Zeki's V3 with squares. Note that at similar eccentricities the receptive fields in V2 are slightly larger than those in V1 and considerably smaller than those in the region anterior to V2. As in the previous figure, the topographic progression is less precise in V2 than in V1.

Figure 6 illustrates the posterior and anterior borders of V2 on the ventral surface in an area representing the central 5° of the upper visual field. Moving within V2 away from the representation of the vertical meridian (site 1 to site 5) the receptive fields move from the vertical meridian toward the horizontal meridian.

At site 6 we have moved out of V2 into another retinotopically organized region. It contains a representation of the upper visual field independent from that in V2. Within this area, the receptive field progression reverses and the field centers move systematically from the horizontal meridian into the periphery (sites 6–12). The location and topography of this area on the ventral border of V2 corresponds to the ventral portion of V3 proposed by Zeki ('74) and to the Ventral Posterior (VP) area described by Newsome et al. ('81). In this and subsequent figures, we have marked receptive field centers that appear to fall within VP with triangles. (Although in this animal we had no recording sites between site 5 and site 6 in the anterior border of V2, the corresponding cortex in other animals contained a representation of the horizontal meridian and 2° of the lower visual field. This incursion into the lower visual field is discussed below.)

The previous three figures showed the progression of receptive fields in the central portion of V2. Figure 7 shows the progression in

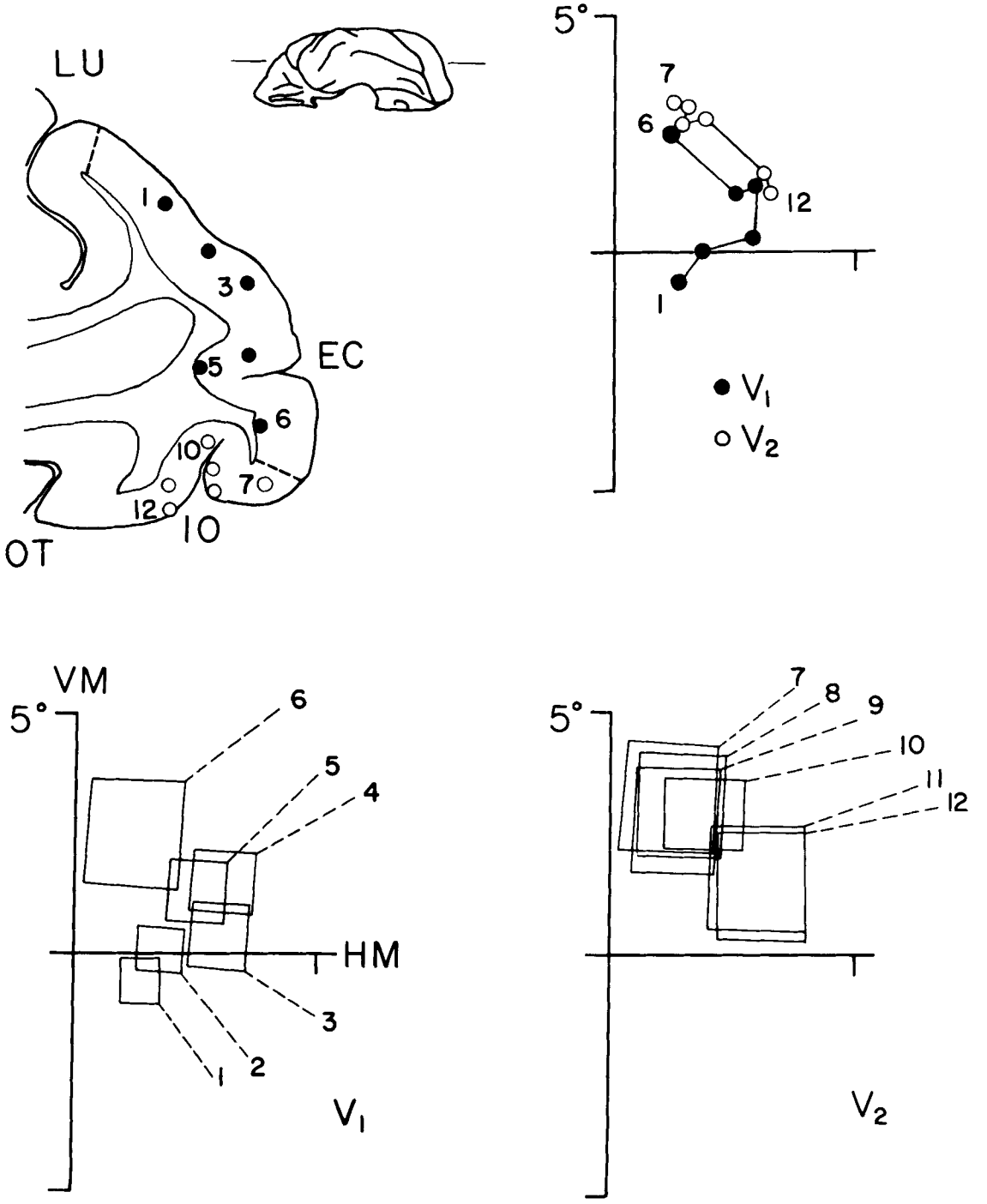


Fig. 4. Central receptive fields in V1 and V2. The recording sites are indicated by circles on the sagittal section (cut at the level indicated on the ventral view of the brain). The location of the centers of the receptive fields recorded at these sites are shown in the upper right and the receptive fields in the lower left (V1) and right (V2). The dashed lines on the section indicate the borders of V2. See also legend to Figure 1.

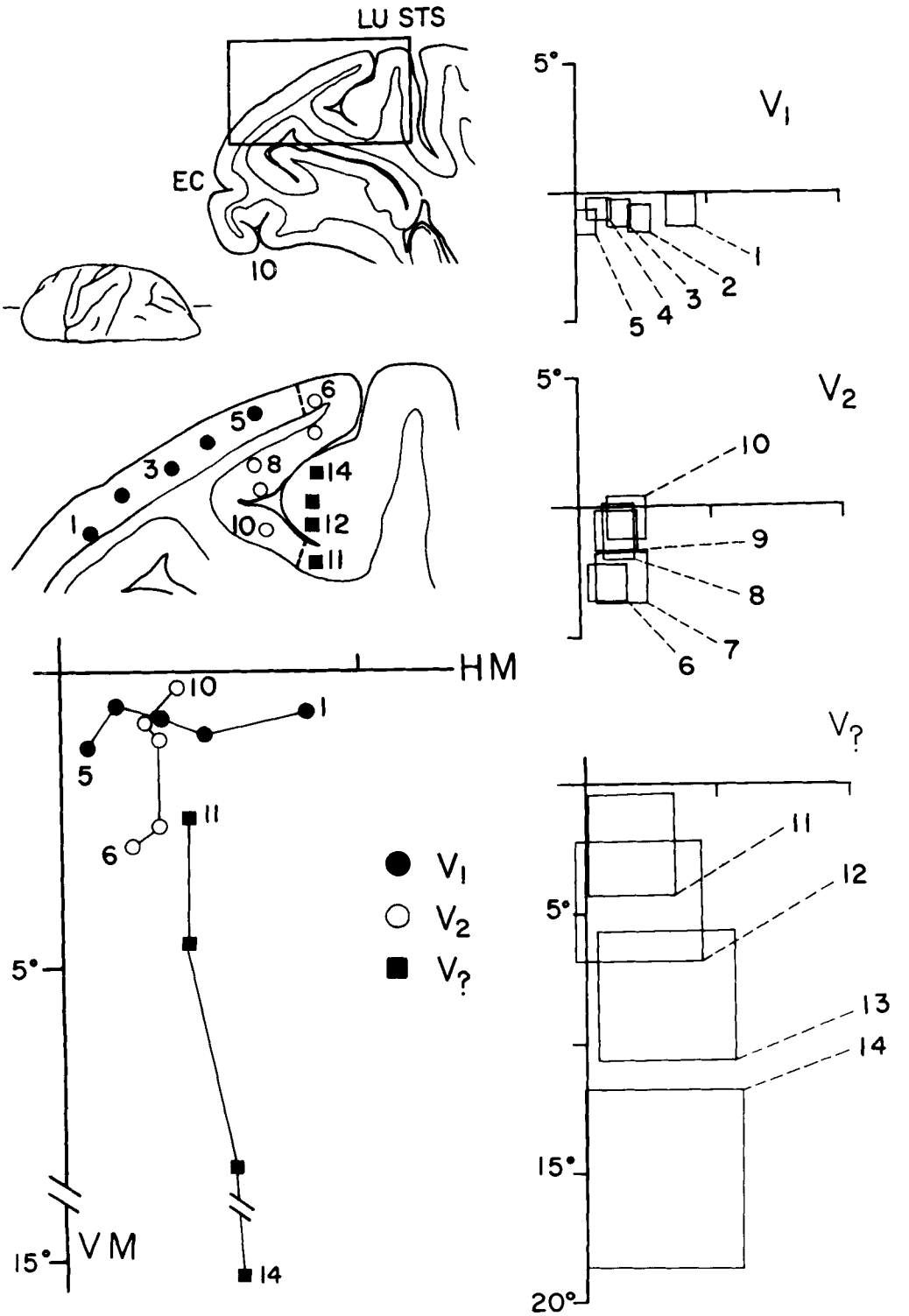


Fig. 5. Central receptive fields in dorsal V1, V2, and an area anterior to V2. The recording sites are indicated on the enlarged sagittal section (cut at the level indicated on the dorsal view of the brain). See also legend to Figures 1 and 4.

the representation of the periphery in V2. Starting at site 1 near the ventral border of V2 and moving to site 6 near the V2/V1 border, the receptive fields move from the horizontal meridian to the vertical meridian in the upper visual field. Crossing into striate cortex at site 7 and moving through V1 in the calcarine sulcus to site 19, the receptive field progression reverses and moves from the vertical meridian in the upper field through the horizontal meridian of V1 to the vertical meridian in the lower visual field. Crossing the V1/V2 border at the upper bank of the calcarine sulcus and moving dorsally along the medial surface of the hemisphere (sites 20–26), the receptive field progression reverses again and moves from the vertical meridian in the lower visual field (site 20) to the horizontal meridian that forms the anterior border of V2 (site 26). Thus, the representation of the upper visual field in V2 borders that of the upper visual field in V1, and, similarly, the representation of the lower fields in V2 and V1 are adjacent. Note that, in the ventral portion of V2 (representing the

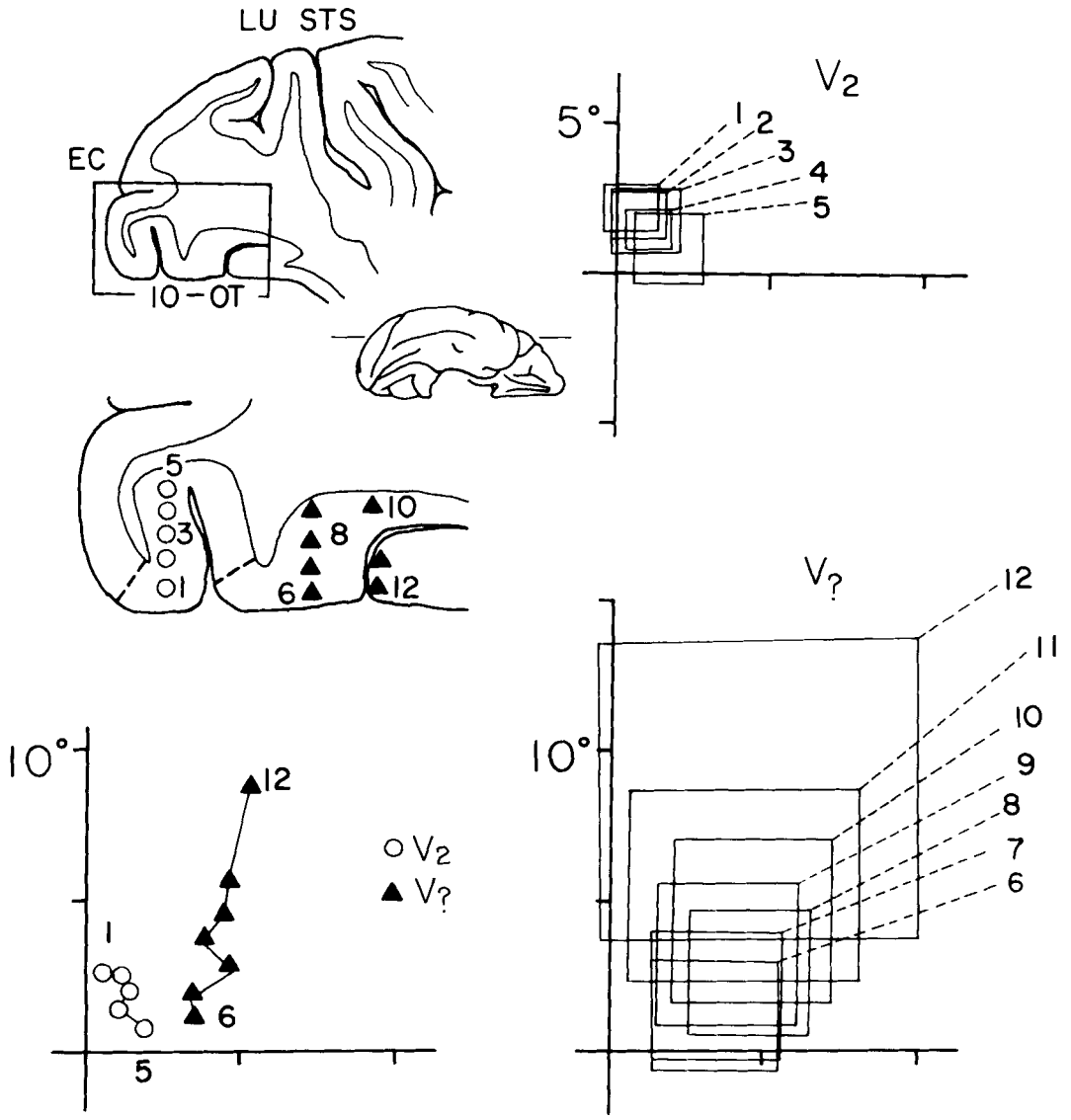


Fig. 6. Central receptive fields in ventral V2 and an area anterior to V2. See also legends for *Figures 1 and 4*.

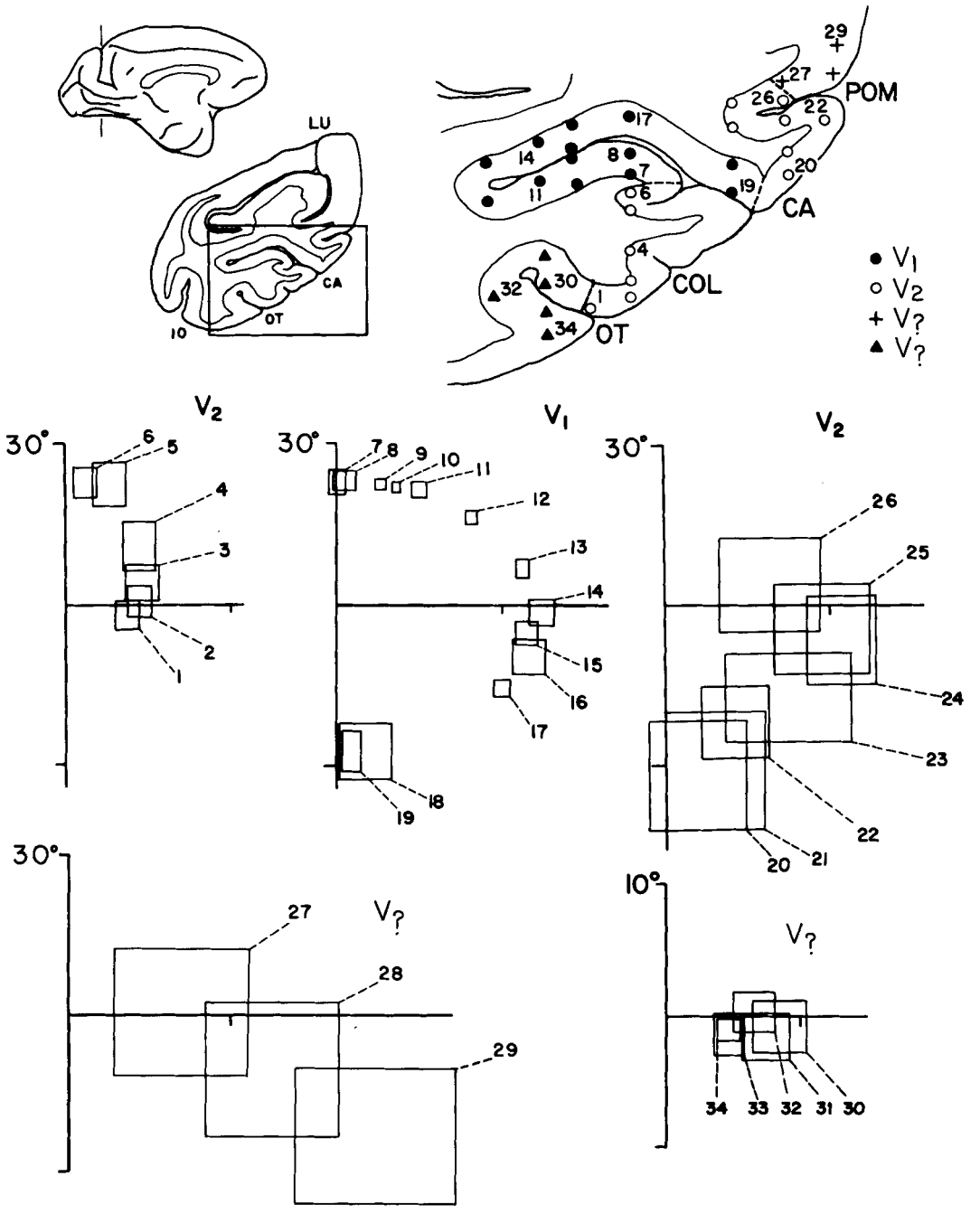


Fig. 7. Peripheral receptive fields in V1, V2, and adjacent areas. See also legends to Figures 1 and 4.

upper visual field), the receptive field centers at the anterior border actually extend a few degrees below the horizontal meridian (field 1). Similarly, in the dorsal portion of V2 (representing the lower visual field), the receptive field centers at the anterior border extend a few degrees above the horizontal meridian (field 26). As in the central representations, the receptive field areas in V2 are larger than those in V1 at similar eccentricities.

There are topographically organized visual areas adjacent to V2 both medially and ventrally. On the medial surface moving from site 26 to site 27 and across the representation of the horizontal meridian and out of V2, the progression of receptive fields reverses and the fields move from the horizontal meridian into the periphery of the lower field (sites 27–29). This appears to be part of a retinotopically organized area that extends into the parieto-occipital sulcus and has not been previously described in the macaque. On the ventral surface, as we enter the occipitotemporal sulcus (site 30), the receptive fields move along the horizontal meridian toward the fovea (sites 30–34). This area seems to be part of the ventral area anterior to V2 shown previously in Figure 6.

In summary, in both the representation of the central 3°–5° and of the periphery, there is a reversal of receptive field progression both as we move across the representation of the vertical meridian forming the posterior border of V2 into V1 and as we move across the representation of the horizontal meridian forming the anterior border of V2.

*Visuotopic organization of V2.* The visual topography of V2 (Fig. 1) was derived by correlating receptive field locations and recording sites in seven monkeys. In this portion of the paper we illustrate these correlations in two coronal sections chosen from one animal and three parasagittal sections chosen from another.

Figure 8 illustrates the posterior coronal section. V2 is located on the ventral surface in the lip of the lower bank of the calcarine sulcus, in a small portion of the medial surface near the upper bank of the calcarine sulcus (which was not recorded from in this animal), and in islands of gray matter that are the posterior tips of the lunate and parieto-occipital sulci. In V1, the receptive field progressions conform to previous descriptions (Talbot and Marshall, '41; Daniel and Whitteridge, '61). Moving dorsally on the lateral surface (sites 1–8) the receptive fields move from the horizontal meridian near the fovea into the lower field. Moving down the upper bank of the calcarine sulcus (sites 43–46) and along its floor (sites 11–15), the receptive fields move toward the horizontal meridian. Continuing along the floor (sites 16–19) and continuing up the lower bank of the calcarine (sites 20–25) toward the medial V2/V1 border near the lower lip of the calcarine sulcus, the receptive fields move from the horizontal meridian toward the vertical meridian.

Crossing the border of V1 with V2 in the lower bank of the calcarine sulcus and moving around the ventral convexity (sites 26–40), the progression of the receptive fields reverses and moves away from the vertical meridian in the upper visual field. It then curves back and moves toward the horizontal meridian near the fovea at the border with striate cortex on the lateral surface.

The islands of cortex from the lunate sulcus (sites 48–52) and the parieto-occipital sulcus (sites 9–10, 41–42) contain portions of the V2 progressions in the lower visual field that become clearer in subsequent sections. Note that the more medial islands contain representations of more peripheral portions of the visual field.

In the more anterior section (Fig. 9), V1 is now restricted to the dorsolateral surface and to the calcarine fissure and there is now considerable V2 cortex both on the ventral surface and in the lunate and parieto-occipital sulci which have expanded from the last section. As in the last section, moving dorsally in V1 along the lateral surface (sites 1–6), the receptive fields move from the fovea into the lower visual field. Again moving in the calcarine sulcus from the upper to the lower bank (sites 26–43), the receptive fields move from the vertical meridian in the periphery of the lower visual field, through the horizontal meridian, to the vertical meridian in the upper visual field but at a greater eccentricity than in Figure 8.

Crossing from V1 to V2 on the dorsal surface, the progression of receptive fields does not reverse as it did in the sagittal sections (Figs. 4, 5). Rather, because this coronal section is almost parallel to the V1/V2 border, moving from lateral to medial along the dorsal convexity, the progression in both areas (V1, sites 1–6 and V2, 7–11) moves inferiorly along the vertical meridian.

The progression of receptive fields in V2 on the medial and ventral surfaces (sites 44–61) is similar to that in the previous figure but at a greater eccentricity, i.e., after crossing into

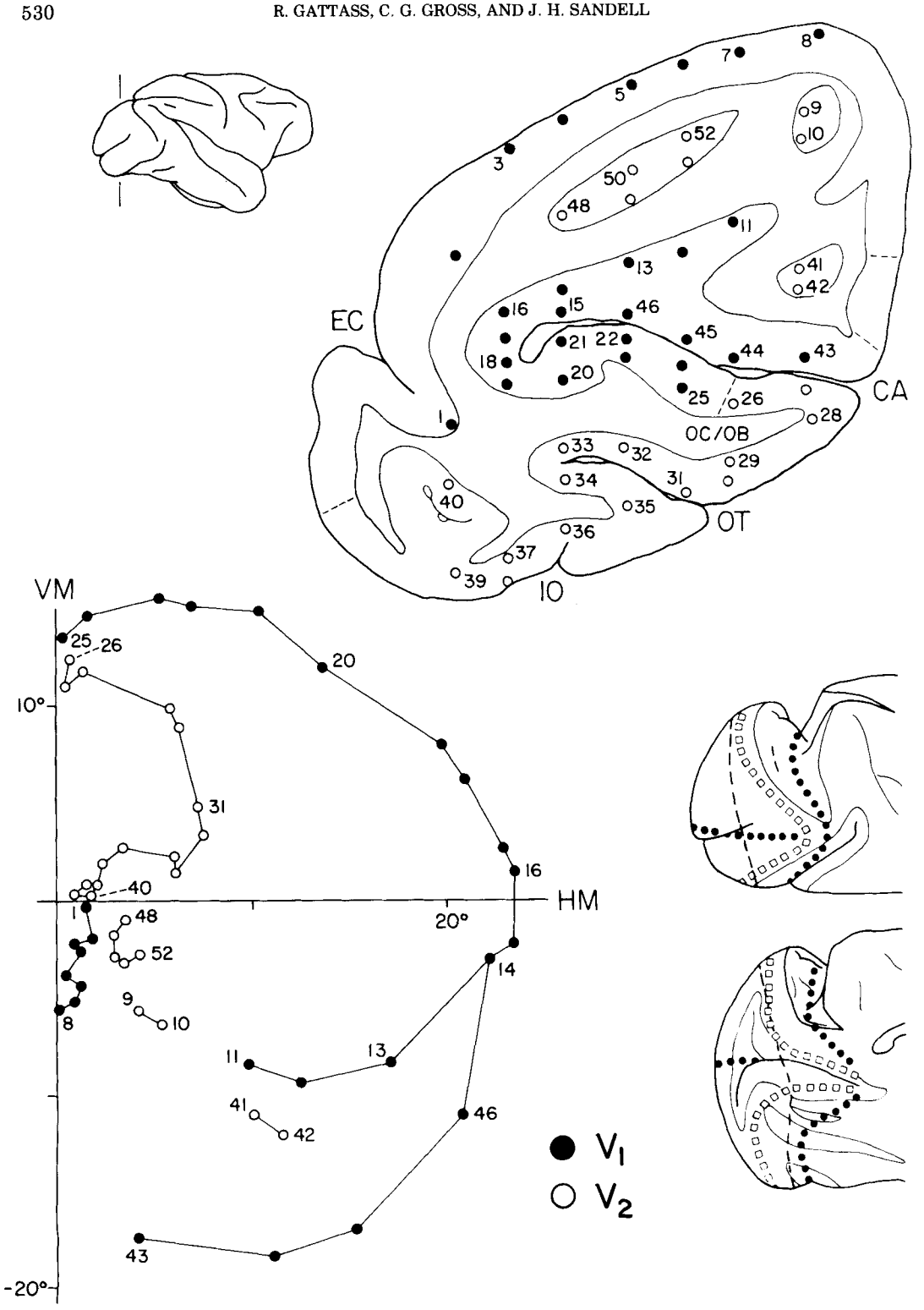


Fig. 8. Location of receptive field centers (lower left) in V1 and V2 recorded at the sites indicated in the coronal section (upper right). The drawings in the lower right show the vertical meridian (squares), the horizontal meridian (filled circles), and the plane of section (dashed lines) in brains with the sulci partially opened. See also legends to Figures 1 and 4.

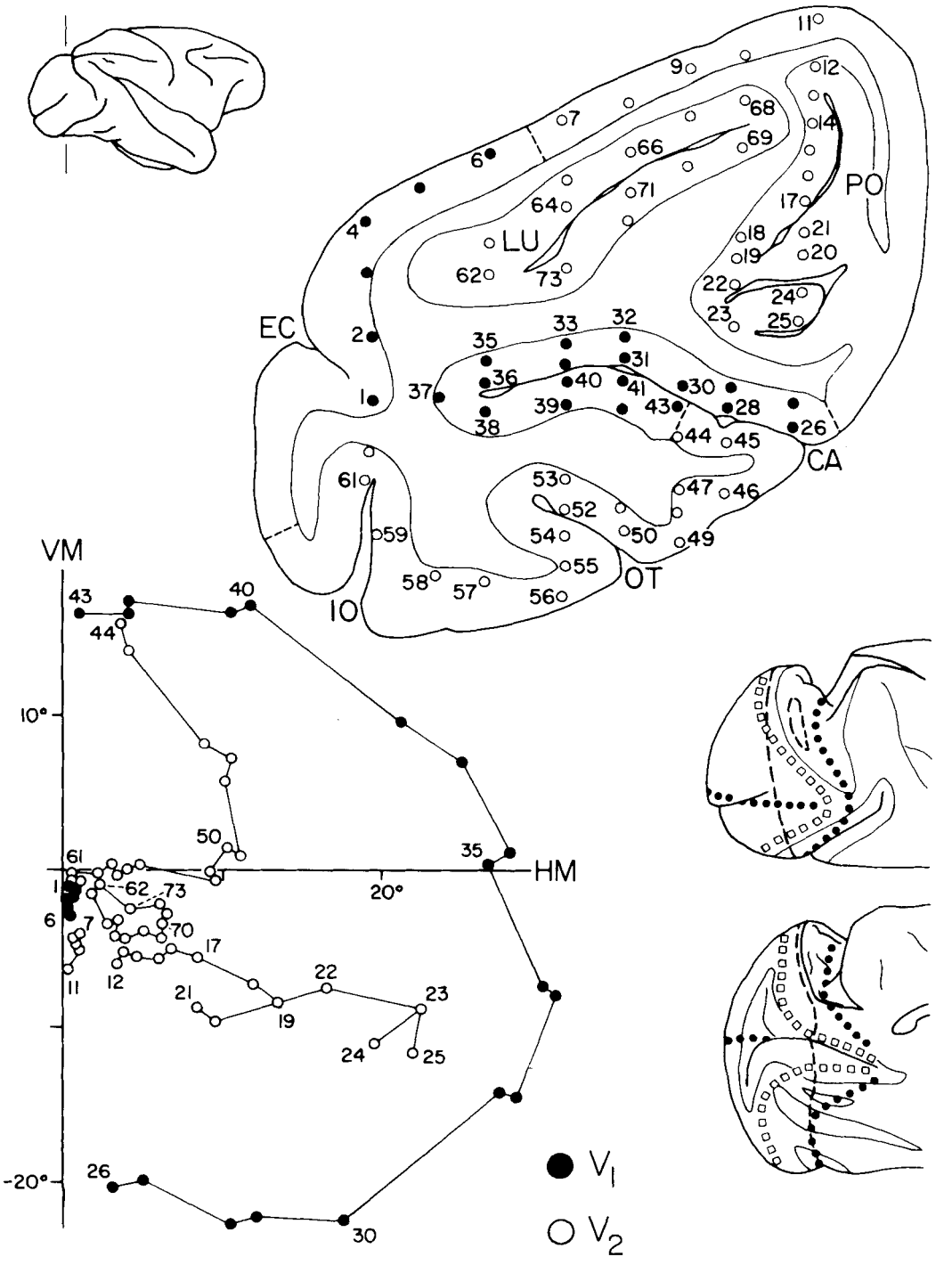


Fig. 9. Location of receptive field centers recorded in V1 and V2 at the sites indicated in the coronal section (which is anterior to the section Fig. 8). See also legend to Figure 8.

V2 at the lower lip of the calcarine (site 44), the fields move out from the vertical meridian in the upper visual field and loop down to the fovea (sites 45–61). Note that the receptive field centers at sites 51–61 run along the horizontal meridian. In fact all of these receptive fields extend about 2° into the inferior visual field. This incursion of about 2° into the lower visual field by the receptive fields in ventral V2 was also seen in Figure 7 and was previously reported by Van Essen and Zeki ('78).

The lunate sulcus is much larger in this section than in the previous one and still contains only V2. The progression of receptive fields around this sulcus (sites 62–73) forms a loop enclosing most of the fields recorded in lunate in the more posterior sections. Similarly, the larger parieto-occipital sulcus contains a continuation of the V2 progression seen in the previous section. Note that, moving medially in the lunate and ventrally in the parieto-occipital sulci, the fields systematically move into the periphery.

The receptive field progressions on the medial surface in a more anterior section from this same animal were shown previously in Figure 7.

Figures 10–12 illustrate receptive fields and recording sites in V2 in a brain cut in sagittal sections. Receptive fields from V1 and from the areas anterior to V2 have been omitted, except for sites immediately adjacent to V2.

In the most lateral section, Figure 10, V2 is found in part of the lower bank of the calcarine sulcus as well as in the posterior bank of the lunate sulcus and on the ventral surface. Crossing from V1 into V2 on the dorsal surface and moving down into the lunate sulcus (sites 3–6), the fields move from the vertical meridian toward the horizontal meridian. Crossing the floor of the lunate sulcus into the annectent gyrus (sites 7–8) we move into another retinotopically organized area and the fields move away from the horizontal meridian toward the periphery (this is probably part of the dorsal portion of Zeki's V3 ['78] [cf. Fig. 5]). Crossing from V1 into V2 in the calcarine sulcus (site 10 to site 11) the receptive field progression reverses. Moving along the lower bank of the calcarine sulcus (sites 11–16) and then through the collateral and inferior occipital sulci (sites 17–26), the receptive fields move in the upper visual field from the vertical meridian into the periphery and then back to the vertical meridian as the ventral border with striate cortex is approached.

In the next, more medial, section, Figure 11, V2 is found in the upper part of the posterior bank of the lunate sulcus, in the ventral bank of the calcarine sulcus, in the parieto-occipital sulcus, and on the ventral convexity. Dorsally, crossing from V1 into V2 and moving down the lunate (sites 3–8), the fields move away from the vertical meridian. Moving into the parieto-occipital cleft (sites 9–10), we move into another retinotopic area (part of Zeki's V3) and, as in the last section (Fig. 10, sites 7–8), the fields move from the horizontal meridian toward the periphery and become much larger. Moving back into V2 at site 11 and moving down the floor of the emerging parieto-occipital sulcus (sites 11–14) the receptive fields move from the horizontal meridian into the periphery. Starting at the V1/V2 border in the lip of the upper calcarine fissure (site 17) and moving toward the anterior border of V2 (sites 18–20), the receptive fields move from the vertical meridian toward the horizontal meridian in the far periphery. Then moving ventrally toward the rostral tip of the calcarine fissure (sites 21–22) the fields move from the horizontal meridian into the periphery. Starting at the V1/V2 border in the lower lip of the calcarine sulcus (site 25) and moving around the collateral sulcus (sites 25–32), the receptive fields move away from the vertical meridian in the upper visual field into the periphery and then back toward the vertical meridian as the ventrolateral border with V1 is approached. This same reversal of progression within V2 was seen in the previous figure but at a greater eccentricity.

In the most medial section, Figure 12, the portion of V2 studied is confined to the posterior bank of the parieto-occipital sulcus and the adjacent ventral cortex. Moving from the dorsal border with V1 to the ventral one (sites 3–13) the fields move in the lower field from the vertical meridian into the periphery and then back to the vertical meridian.

### *Receptive field area and eccentricity*

In two animals, receptive field areas were measured in V1 and V2 with a single electrode, which had constant impedance (1 MΩ) throughout the recordings. The square root of receptive field area as a function of eccentricity is plotted in Figure 13 for both V1 and V2. As noted previously, at a given eccentricity, V2 had larger receptive fields than V1. Straight lines were fitted to the data with the method of least squares, and the slope for V2 (0.40)

was significantly greater than for V1 (0.16) according to a t-test ($t = 11.26$, $P < 0.001$). That is, receptive field size in V2 increases more rapidly with eccentricity than in V1. (It should be noted that in both V1 and V2 the receptive fields recorded with multiunit electrodes tended to be slightly larger than those recorded with single unit electrodes.)

*Cortical magnification and eccentricity*

Cortical magnification, i.e., the distance in millimeters between two recording sites divided by the distance in degrees between the centers of the receptive fields recorded at those sites (Daniel and Whitteridge, '61), was measured as a function of eccentricity for V1 and V2 (Fig. 14). Although cortical magnification appeared slightly greater in V1 than in V2, particularly in the central 10° there was no significant difference between the power functions fitted to the data with the method of least squares ($t = 1.23$). The best fitting power function for V1 was $M = 5.5E^{-1.2}$ and for V2, $M = 4.0E^{-1.1}$ where M is the cortical magnification factor and E, retinal eccentricity. The

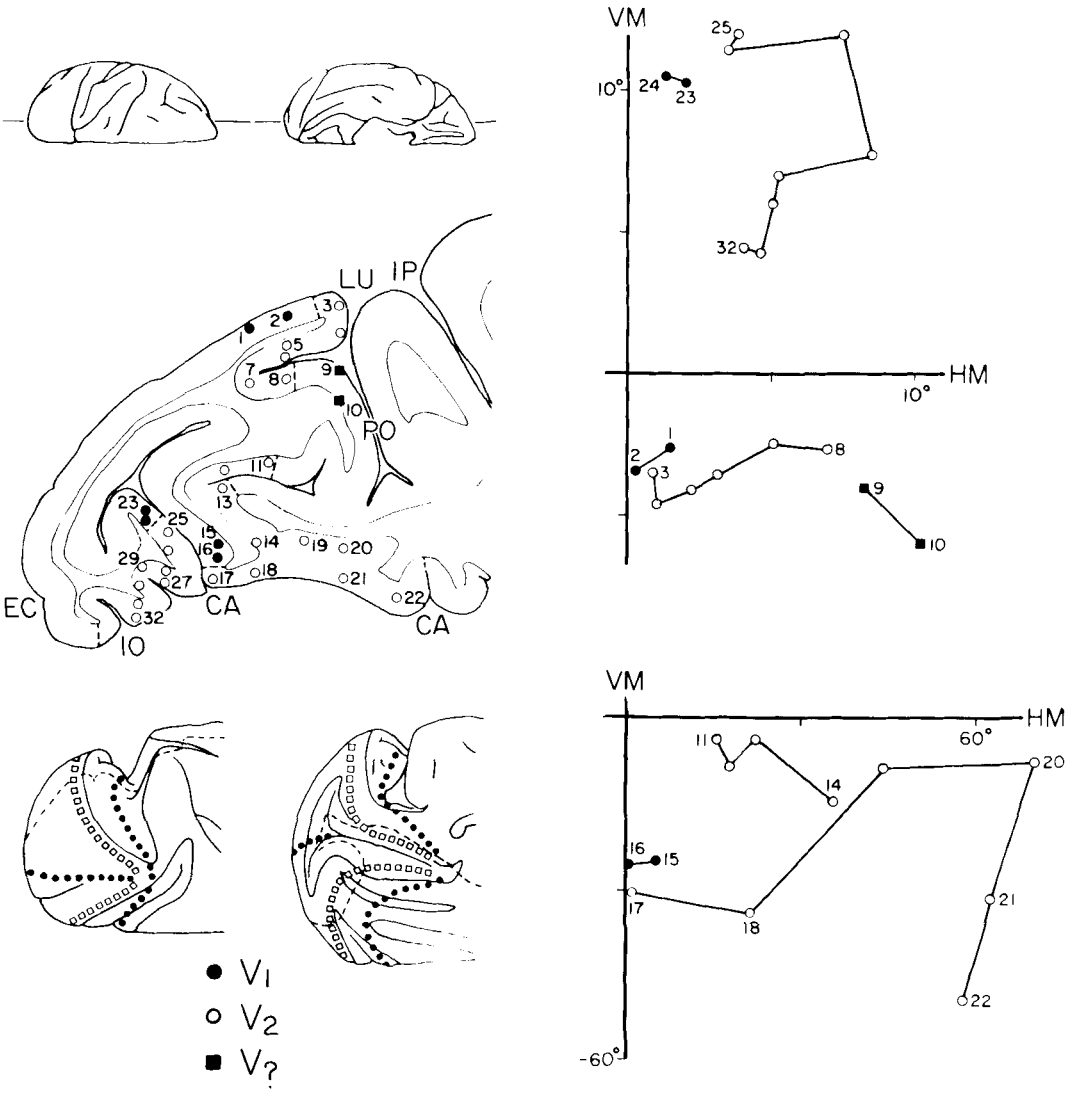


Fig. 10. Location of receptive field centers in V2 recorded at the sites indicated in the parasagittal section (L 10). Receptive field centers in adjacent areas are also indicated. Note that the scale in the right upper graph is larger than that in the right lower one. See also legend to Figure 8.

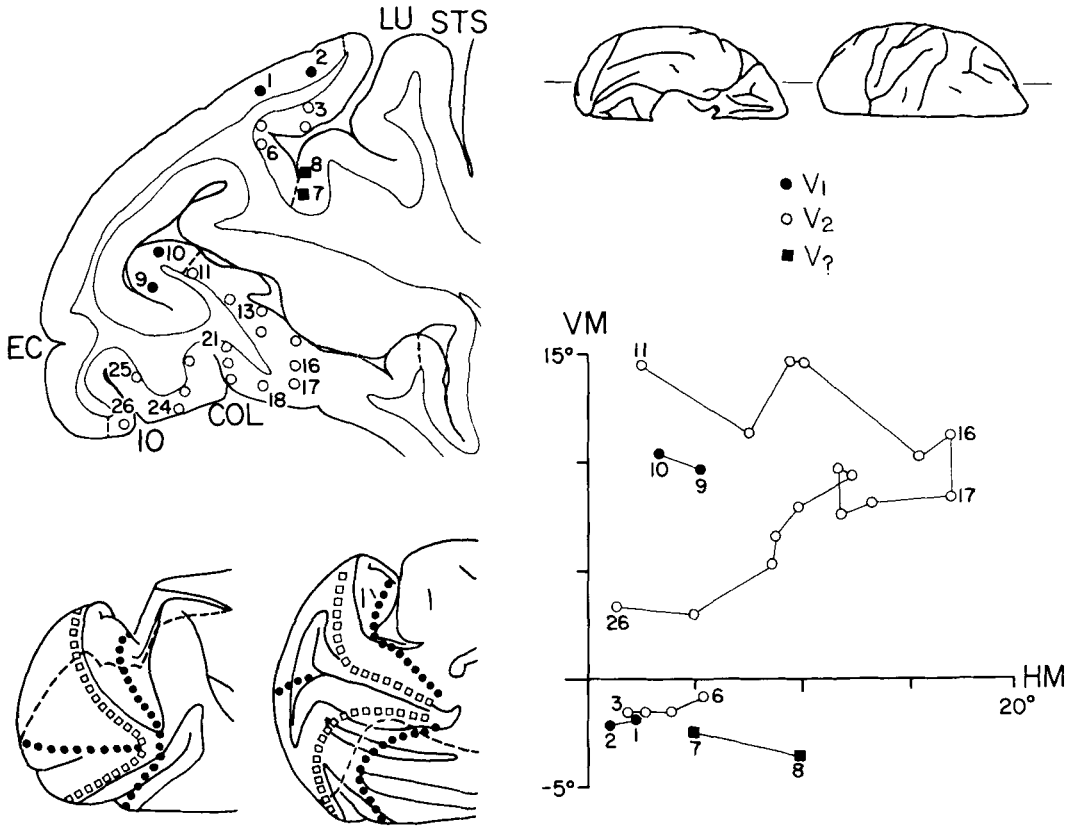


Fig. 11. Location of receptive field centers in V2 recorded at the sites indicated in the parasagittal section. Receptive field centers in adjacent areas are also indicated. See also legend to Figure 8.

function for V1 was similar to that calculated by Schwartz ('77) from Daniel and Whitteridge's ('61) data, i.e., $M = 6.0E^{-0.9}$.

*Architectonic correlates of V2*

In Nissl-stained sections, the border between V1 and V2 was, of course, always clear; it corresponded with the representation of the vertical meridian. We were unable, however, to reliably distinguish the anterior border of V2 on cytoarchitectonic grounds. We were able to distinguish V2 from the areas bordering it anteriorly in sections stained for myelin with the modified Heidenhain-Woelke stain (Gattass and Gross, '81). (But we were unable to do so with either the Weil or Spielmeyer myelin stains.) These myeloarchitectonic distinctions were particularly visible under low-power (× 15) magnifications and are described below and illustrated in Figure 15. However, the border between adjacent myeloarchitectonic areas was sometimes difficult to see, particularly when the cortex was folded.

In Heidenhain-Woelke-stained sections, V2 is characterized by a homogeneous broad dark band of fibers extending from layer VI through layer IV and fading out in layer III. Under high power this homogeneous band appears to be composed chiefly of thick radial fibers. Thinner fibers in various orientations contribute to the homogeneous appearance at low power. There are occasional horizontal bundles of intermediate thickness in the lower layers particularly near the border with VI. The border between the bottom of layer VI and the white matter is sharp.

Since V2, as determined by visual topography, always had these myeloarchitectonic characteristics, we used the myeloarchitecture to determine the border of V2 when this border fell between two recording sites and at the representation of the center of gaze. In general, V2 appeared coextensive with von Bonin and Bailey's ('47) cytoarchitectonic Area OB. One possible difference between von Bonin and Bailey's cytoarchitectonic Area OB and our V2

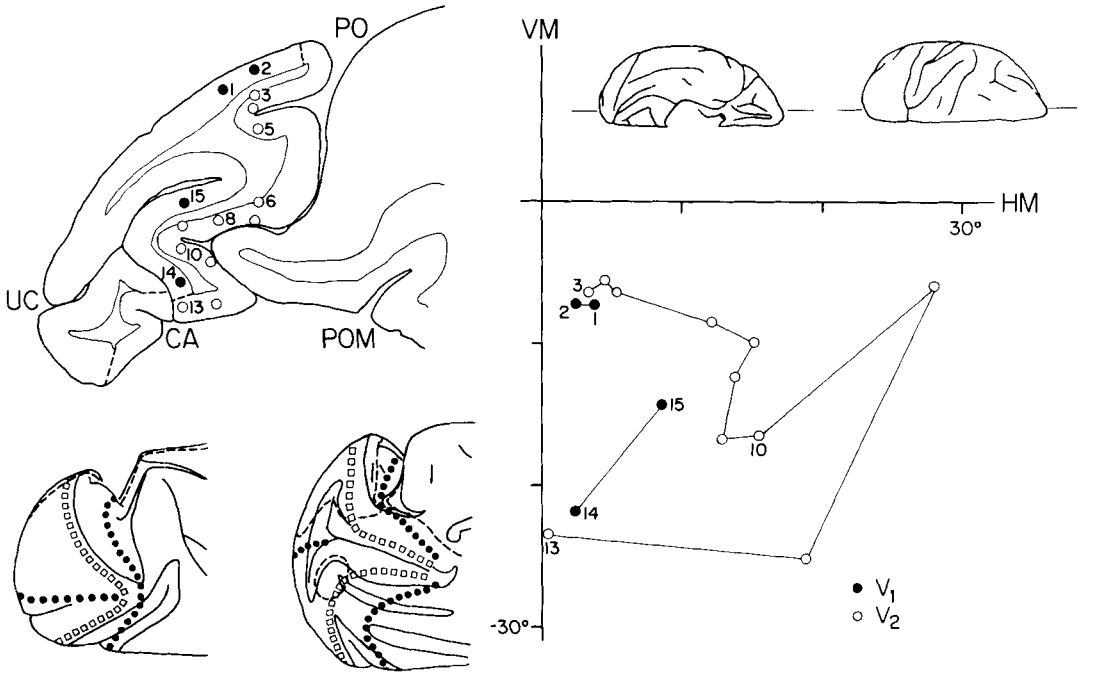


Fig. 12. Location of receptive field centers in V2 recorded at the sites indicated in the parasagittal section. Adjacent field centers in V1 are also indicated. See also legend to Figure 8.

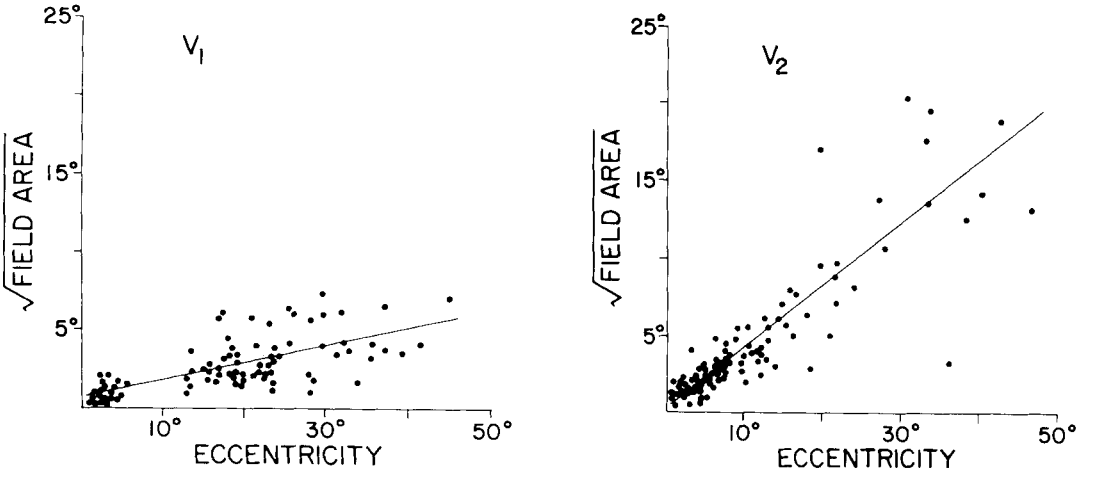


Fig. 13. Square root of receptive field area vs. retinal eccentricity for V1 (left) and V2 (right). Data for both areas were obtained from two animals. The straight lines were fitted with the method of least squares.

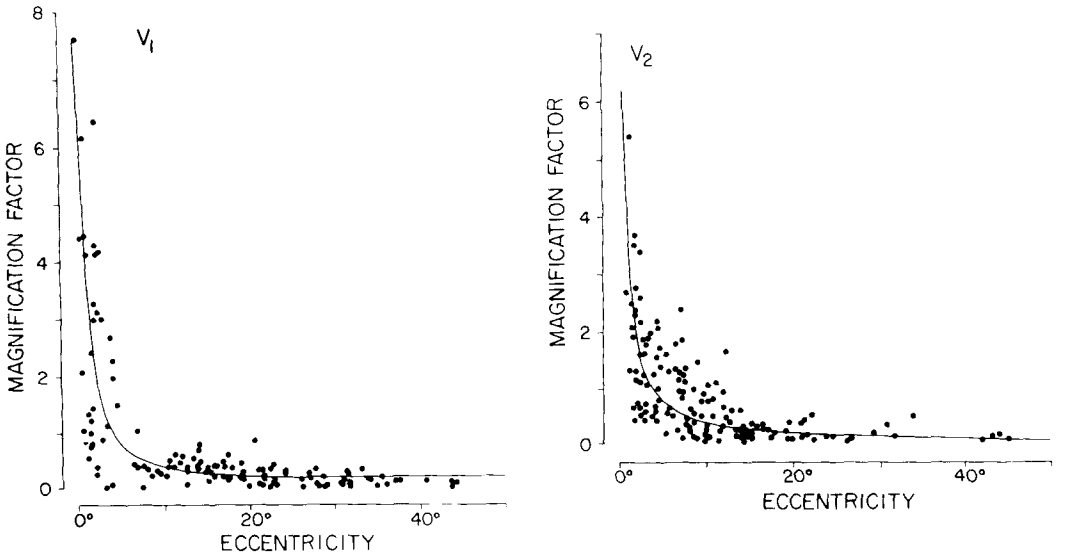


Fig. 14. Magnification factor in mm/degree vs. eccentricity for V1 (left) and V2 (right). Data for both areas were obtained from two animals. The power functions were fitted with the method of least squares.

was at the extreme rostral end of the calcarine fissure anterior to striate cortex. Von Bonin and Bailey label this Area OB but we found the myeloarchitectonic pattern to be different from that of V2 and from the other areas bordering V2. It may correspond to Area Prostriata of Sanides ('70). We had no recording sites in this region.

Although V2 was myeloarchitectonically different from the adjacent cortex, we did find myeloarchitectonically similar cortex elsewhere in prestriate cortex. One such site was the striate projection zone in the posterior superior temporal sulcus also known as MT (Gattass and Gross, '81; Van Essen et al., '81); the other was in the intraparietal sulcus.

The cortex immediately anterior to V2 is not homogeneous in appearance. Common to all of it, however, is a more stratified and less homogeneous appearance of the lower layers in Heidenhain-Woelke-stained sections.

## DISCUSSION

### *Organization of V2*

We have described the topographic organization of V2 in the macaque. It contains a complete topographically organized representation of the contralateral visual field. The representation of the vertical meridian in V2 is adjacent to that in striate cortex and forms the posterior border of V2. Thus, V2 surrounds V1 except at the most rostral millimeter or two of V1 in the anterior tip of the calcarine sulcus (see Fig. 1). The representation of the horizontal meridian in V2 forms the anterior border of V2 with the representation of the lower visual field located dorsally and that of the upper visual field ventrally. Thus, two nearby points on either side of the horizontal meridian of the visual field may be represented in distant sites in V2. This type of representation of the visual field has been called a second-order transformation (Allman and Kaas, '74) and is characteristic of V2 in the cat (Tusa et al., '79) and at least two other primates—galago (Kaas, '80) and owl monkey (Allman and Kaas, '74). Finally, the representation of the central 1° in V2 is opposite that in V1. With our methods it was not possible to locate precisely the representation of the horizontal meridian within the representation of the central 1° in V2. There was a tendency, however, for sites with receptive field centers less than 1° above the horizontal meridian to be located, on the average, more ventrally than sites with receptive field centers less than 1° below the horizontal meridian. Thus, the horizontal meridian appears to be contiguous with that in V1 but then splits at about 1° from the center of gaze and forms the anterior border of V2.

In the cat, galago, and owl monkey, the representation of the horizontal meridian in V2 is also contiguous with that in V1 but in these species, it splits 5°–7° from the center of gaze

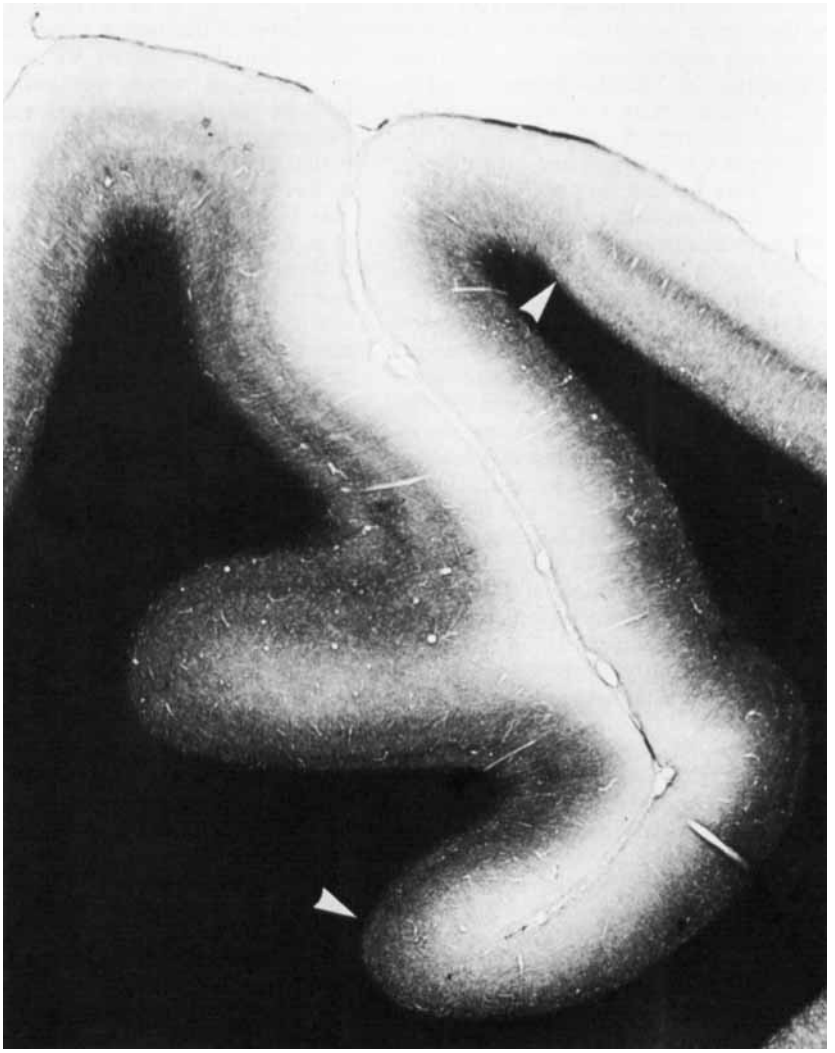

Fig. 15. Microphotograph (× 13) of a parasagittal section through the lunate sulcus showing V2 (between arrows).

and then forms the anterior border of V2 (Tusa et al., '79; Kaas, '80; Allman and Kaas, '74). The more central splitting of the horizontal meridian in the macaque may be related to its greater cortical magnification in the foveal representation and the highly specialized fovea of the macaque, absent in the other three species.

V2 is at least several times larger than any other cortical area receiving a direct striate input. Indeed, it is only slightly smaller than V1 itself. Thus, V2 is presumbably the principal source of information for subsequent stages of visual processing. Allman and Kaas ('74) have proposed that its second-order transformation of the visual field affords close connection between representation of corresponding points in the visual field in V1 and V2. They further suggest that V1 and V2 may form a functional dyad (Allman and Kaas, '74). This idea is supported by our finding that both cortical magnification and the area of the visual field represented were very similar in V1 and V2. Indeed, the only major differences we

found between the visual topography in V1 and V2 were the larger receptive fields in V2 and the considerably greater scatter or coarseness in the topography of V2. The larger receptive fields in V2, also noted by Van Essen and Zeki ('78), presumably reflect convergence of the projections from V1. The less fine-grain topography of V2 may be due, in part, to this convergence. It is also probably related to the finding that single injections of $^3$H proline in V1 show projections to several adjacent patches in V2 (e.g., Weller and Kaas, '81).

Several previous investigators have provided information about the topographic organization of V2. On the basis of anatomical experiments, Zeki ('69, '77; Zeki and Sandeman, '76) and Cragg ('69) located the representation of the vertical meridian of V2 along its border with V1 and the representation of the horizontal meridian, at least out to 30°, at its anterior border. Zeki and Sandeman ('76) and Van Essen and Zeki ('78) recorded single neurons in the posterior bank of the lunate sulcus and demonstrated an organized representation of about the central 10° of the lower visual field. More recently, the projections from both the central and peripheral representation in striate cortex to V2 were studied by Rockland and Pandya ('81), Ungerleider and Mishkin ('79), and Weller and Kaas ('81). The topography of V2 indicated in these studies appears consistent with that presented in this report.

V2 was myeloarchitectonically distinguishable from surrounding areas. To within a few millimeters, our location for V2 was coextensive with cytoarchitectonic Area OB of von Bonin and Bailey except in the most rostral portion of the calcarine sulcus, as noted in Results. Again to within a few millimeters, our V2 was similar to the striate-recipient zone adjacent to V1 described by several authors (Zeki, '69; Cragg, '69; Rockland and Pandya, '81; Ungerleider and Mishkin, '79) on the basis of anterograde anatomical methods.

In the owl monkey the visual topography and anatomical connections of at least seven visual areas anterior to V2 have been described by Allman and Kaas and their colleagues (see reviews by Kaas, '80; Allman, '81; Weller and Kaas, '81). In the macaque, the situation is less clear. The topography of only one visual area anterior to V2 has been described in detail, namely MT, a striate projection zone in the posterior portion of the superior temporal sulcus (Gattass and Gross, '81; Van Essen et al., '81). The present results confirm Newsome et al.'s ('81) report of a representation of the upper visual field ventral to V2 which they named VP and which corresponds to the ventral portion of V3, proposed by Zeki ('74). Our results also confirm the dorsal portion of Zeki's V3; namely a representation of the lower visual field bordering V2 in the lunate sulcus reported by Zeki ('75, '77, '78), Van Essen and Zeki ('78), and Van Essen et al. ('79). Finally, there appears to be at least a third topographically organized area anterior to V1. It lies medial to V2 and extends into the parieto-occipital sulcus. Considerable additional work will be required to untangle further the organization and relations of prestriate visual areas in the macaque.

ACKNOWLEDGMENTS

We thank V. Ingalls and S. Gorlick for assistance with the histology, R. Desimone, T. Albright, A.P.B. Sousa, L. Ungerleider, M. Mishkin, E. Covey, D. Van Essen, and J. Allman for their comments on the manuscript, D. Dawson for help with the figures, J. Kaas for information on the Heidenhain-Woelke stain, K. Walsh for typing, and the National Institute of Health (MH-19420 and FO5TW02855), the National Science Foundation (BNS 79-05589), and the Conselho Nacional de Desenvolvimento Cientifico e Tecnologico-Brasil (CNPq 1112.1003/77) for financial assistance.

LITERATURE CITED

Allman, J. M. (1981) Reconstructing the evolution of the brain in primates through the use of comparative neurophysiological and neuroanatomical data. In E. Armstrong (ed): Primate Brain Evolution: Methods and Concepts. New York: Plenum Press.

Allman, J. M., and J. H. Kaas (1974) The organization of the second visual area (VII) in the owl monkey: A second order transformation of the visual field. Brain Res. *76*:247–265.

Cowey, A. (1964) The projection of the retina on to striate and prestriate cortex in the squirrel monkey *Saimiri sciurens*. J. Neurophysiol. *27*:366–393.

Cragg, B. G. (1969) The topography of the afferent projections in the circumstriate visual cortex of the monkey studied by the Nauta method. Vis. Res. *9*:733–747.

Daniel, P. M., and D. Whitteridge (1961) The representation of the visual field on the cerebral cortex in monkeys. J. Physiol. (Lond.) *159*:203–221.

Desimone, R., and C. G. Gross (1979) Visual areas in the temporal cortex of the macaque. Brain Res. *178*:363–380.

Gattass, R., and C. G. Gross (1981) Visual topography of the striate projection zone in the posterior superior temporal sulcus (MT) of the macaque. J. Neurophysiol. *46*:621–638.

Gattass, R., C. G. Gross, and J. H. Sandell (1979) V2 in the macaque: Visuotopic organization and extent. Neurosci. Abstr. *5*:786.

Hubel, D. H., and T. N. Wiesel (1965) Receptive fields and functional architecture in two nonstriate visual areas (18 and 19) of the cat. J. Neurophysiol. *28*:229–289.

Kaas, J. H. (1980) A comparative survey of visual cortex organization in mammals. In S. O. E. Ebbesson (ed): Comparative Neurology of the Telecephalon. New York: Plenum Press, pp. 483–502.

Kaas, J. H., R. W. Guillery, and J. M. Allman (1972) Some principles of organization in the dorsal lateral geniculate nucleus. Brain Behav. Evol. *6*:253–299.

Lillie, R. D. (1965) Histopathologic Technic and Practical Histochemistry. New York: McGraw-Hill, pp. 490–491.

Malpeli, J. G., and F. H. Baker (1975) The representation of the visual field in the lateral geniculate nucleus of *Macaca mulatta*. J. Comp. Neurol. *161*:569–594.

Newsome, W. T., J. H. R. Maunsell, and D. C. Van Essen (1980) Areal boundaries and topographic organization of Ventral Posterior area (VP) of the macaque monkey. Exp. Brain Res. *41*:A21–A22 (Abstract).

Rockland, K. S., and D. N. Pandya (1981) Cortical connections of the occipital lobe in the rhesus monkey: Interconnection between areas 17, 18, 19 and the superior temporal sulcus. Brain Res. *212*:249–270.

Sanides, F. (1970) Functional architecture of motor and sensory cortices in primate in the light of a new concept of neocortex evolution. In C. R. Noback and W. Montagna (eds): The Primate Brain. New York: Appleton-Century-Crofts, pp. 137–208.

Schwartz, E. L. (1977) Spatial mapping in the primate sensory projection: Analytic structure and relevance to perception. Biol. Cyber. *25*:181–194.

Sousa, A. P. B., R. Gattass, and E. Oswaldo-Cruz (1978) The projection of the opossum's visual field on the cerebral cortex. J. Comp. Neurol. *177*:569–588.

Talbot, S. A. (1942) A lateral localization in cat's visual cortex. Fed. Proc. *1*:84 (Abstract).

Talbot, S. A., and W. H. Marshall (1941) Physiological studies on neural mechanisms of visual localization and discrimination. Am. J. Ophthalmol. *24*:1255–1264.

Tusa, R. J., A. C. Rosenquist, and L. A. Palmer (1979) Retinotopic organization of areas 18 and 19 in the cat. J. Comp. Neurol. *185*:657–678.

Ungerleider, L., and M. Mishkin (1979) Three cortical projection fields of area 17 in the rhesus monkey. Neurosci. Abstr. *5*:812 (Abstract).

Van Essen, D. C., and J. H. R. Maunsell (1980) Two-dimensional maps of the cerebral cortex. J. Comp. Neurol. *191*:255–281.

Van Essen, D. C., J. H. R. Maunsell, and J. L. Bixby (1979) Areal boundaries and topographic organization of visual areas V2 and V3 in the macaque monkey. Neurosci. Abstr. *5*:812 (Abstract).

Van Essen, D. C., J. H. R. Maunsell, and J. L. Bixby (1981) The middle temporal visual area in the Macaque: Myeloarchitecture, connections, functional properties and topographic connections. J. Comp. Neurol. *199*:293–326.

Van Essen, D. C., and S. M. Zeki (1978) The topographic organization of rhesus monkey prestriate cortex. J. Physiol. (Lond.) *277*:193–226.

Von Bonin, G., and P. Bailey (1947) The Neocortex of *Macaca mulatta*. Urbana: University of Illinois Press.

Weil, A. (1945) Textbook of Neuropathology. New York: Grune and Stratton, pp. *328–329*.

Weller, R. E., and J. Kaas (1981) Cortical and subcortical connections of visual cortex in primates. In C. Woolsey (ed): Cortical Sensory Organization. Clifton, N. J.: Humana Press, in press.

Zeki, S. M. (1969) Representation of central visual fields in prestriate cortex of monkey. Brain Res. *14*:271–291.

Zeki, S. M. (1974) The mosaic organization of the visual cortex in the monkey. In R. Bellairs and E. G. Grey (eds): Essays on the nervous system. Oxford: Oxford University Press, pp. 327–343.

Zeki, S. M. (1975) The functional organization of projections from striate to prestriate visual cortex in the rhesus monkey. Cold Spring Harbor Symp. Quant. Biol., *40*:591–600.

Zeki, S. M. (1977) Simultaneous anatomical demonstration of the representation of the vertical and horizontal meridians in areas V2 and V3 of rhesus monkey visual cortex. Proc. R. Soc. Lond. (Biol.) *195*:517–523.

Zeki, S. M. (1978) The third visual complex of rhesus monkey prestriate cortex. J. Physiol. (Lond.) *277*:245–272.

Zeki, S. M., and D. R. Sandeman (1976) Combined anatomical and electrophysiological studies on the boundary between the second and third visual areas of the rhesus monkey cortex. Proc. R. Soc. Lond. (Biol.) *194*:555–562.